

Supporting Information

In situ Surface-Enhanced Raman Spectroelectrochemical System with a Hemin Modified Nanostructured Gold Surface

Tao Yuan^{†,¶}, Loan Le Thi Ngoc^{‡,¶}, Jan van Nieuwkastele[‡], Mathieu Odijk[‡], Albert van den Berg[‡], Hjalmar Permentier[†], Rainer Bischoff[†], Edwin T. Carlen^{‡,§,*}

[†]Analytical Biochemistry and Department of Pharmacy, University of Groningen
Deusinglaan 1, 9713 AV, Groningen, The Netherlands

[‡]MESA+ Institute for Nanotechnology, University of Twente
Drienerlolaan 5, 7522 NB, Enschede, The Netherlands

[§]Graduate School of Pure and Applied Sciences, University of Tsukuba
1-1-1 Tennodai, Tsukuba, Ibaraki 305-8573, Japan

[¶]Authors contributed equally to this work

*Email: ecarlen@ims.tsukuba.ac.jp

SEC chip fabrication. Figure S1 shows the SEC chips fabrication process. A 40 nm thick low stress silicon nitride (SiN) layer was first deposited onto the silicon wafer by low-pressure chemical vapor deposition (Fig. S1(a)). Next, a positive photoresist was spin-coated on the SiN layer and patterned with conventional contact ultraviolet lithography, and subsequently developed. After the development step, a 5 nm Cr and 100 nm Pt metal stack was deposited on the wafer by sputtering, and followed by a lift-off process with acetone, ultrasonication, and rinsing with deionized water (Fig. S1(b)). There was a 1.5 mm separation gap at the center of the chip between the Pt electrodes where the nanostructured WE was to be fabricated. The wafer was then cut into 5 pieces (chips). The chips were then cleaned in a 3:1 mixture of piranha (H₂SO₄:30% H₂O₂). The nanopatterned SiN template surfaces were then formed over a 0.5×0.5 mm² area at the center of the chip between the Pt electrodes (Figs. S1(c)-S1(e)) (see the details of the fabrication of the nanostructured gold surface in the following section). The final step of the SEC chip fabrication was the deposition of the nanostructured Au WE. A custom-made shadow mask (0.1 mm thick sheet of Ni) with a square hole (1 mm²) at its center was used to selectively deposit Au on the nanopatterned SiN region to form the nanostructured Au WE. A 60 nm Au layer, (with a thin Ti adhesion layer to prevent delamination,) was deposited (sputtering with DC source in Ar plasma) on the SiN template to form the SERS-active WE. The Au layer partially overlaps one of the Pt electrodes for external electrical connection to the potentiostat (Fig. S1(f) and S1(g)). The Ti adhesion layer is very thin (deposition rate: 0.06 nm s⁻¹ and deposition time: 3

s.) to prevent plasmon damping. The microfluidic chamber was fabricated from a 3 mm thick layer of polydimethylsiloxane (PDMS). A 3 mm diameter hole was punched ($\phi 3.0$ mm Unicore, Harris) in the PDMS layer to form a cylindrical well (21 mm^3). The patterned PDMS layer was then bonded to the SEC chip by applying pressure (Fig. S1(h)). The SEC chips can be used multiple times by replacing the Ti/Au WE layer and the PDMS microfluidic chamber.

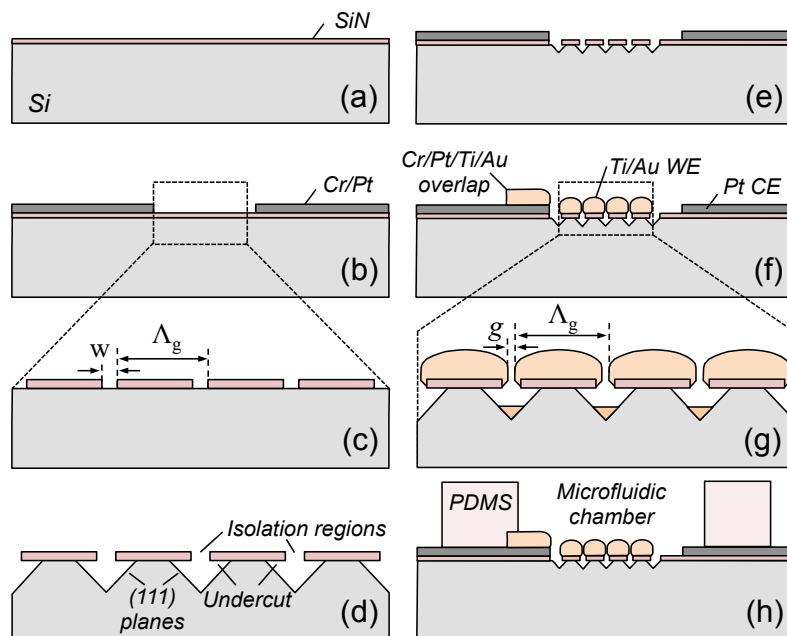


Figure S1. SEC chip fabrication process steps. See text for clarification of the individual steps a to h.

Nanostructured gold working electrode fabrication. A 100 nm polymethyl methacrylate (PMMA, MicroChem Corp.) electron-sensitive photoresist was spin-coated on a silicon substrate and exposed to a 130 pA electron beam with the area dose in the range of $90\text{--}120 \mu\text{A s cm}^{-2}$ (FEI Sirion UHR-SEM). The electron-beam exposure along the length of the SiN template was aligned to the [110] direction of the (100) silicon wafers using the wafer flat as a reference. The total template surface array of 1 mm^2 is written in $0.1 \times 0.1 \text{ mm}^2$ sections. The exposed regions were developed in a 1:3 methyl isobutyl ketone:isopropanol solution for 30 s, followed by immersion in isopropanol. The exposed SiN regions were removed using reactive ion etching (60 W, 25 sccm CHF_3 and 5 sccm O_2), followed by removal of the remaining PMMA and surface cleaning with oxygen plasma. Prior to silicon etching, the native oxide on the exposed silicon regions was removed by immersion in 1% hydrofluoric acid solution for 1 min, and subsequent rinsing with deionized water. The silicon was etched in a 1% KOH solution at 55°C with stirring for 45 s and rinsed with deionized water for 2 min. The different crystal planes etch anisotropically by hydroxide ions in an alkaline solution where (111) planes have the lowest etch rate and (100) and (110) planes both have higher etch rates.¹ The surfaces were then cleaned in a 3:1 piranha solution ($\text{H}_2\text{SO}_4\text{:}30\% \text{H}_2\text{O}_2$) for 15 min, rinsed with deionized water for 2 min, and dried with N_2 . The Ti and Au film stack is

deposited by sputtering (DC source) in an Ar plasma (Au deposition rate: 0.06 nm s⁻¹ and Ti deposition rate: 0.06 nm s⁻¹) deposition.

Working electrode preparation and modification. Two working electrodes were used for the experiments. Electrochemical measurements were performed on the Au disk electrode while the nanostructured Au surface was used for the in situ SEC measurements. A conventional Au disk electrode (Bioanalytical Systems, Inc.) with 1.6 mm diameter was polished with a microcloth (Micromesh Grade 3200) and alumina slurry (ϕ 0.05 μ m particles), and subsequently sonicated in water, ethanol and water, each for 1 min. The Au electrode was then immersed in a 3:1 piranha solution (H₂SO₄:30% H₂O₂), and washed thoroughly with deionized water and dried with N₂. The workflow of the electrode modification is displayed in Fig. S2. First, the Au electrode was immersed in 1 mM 4-mercaptopyridine (MPy) in ethanol for 4 h, followed by 1 min sonication in ethanol. After drying the MPy modified Au electrode with N₂, it was immersed in a hemin solution (1 mM in DMSO) for 18 h. Before use, the hemin modified electrode was sonicated in DMSO and water, each for 1 min. The nanostructured Au WE was modified with the MPy/hemin layer using a similar protocol.

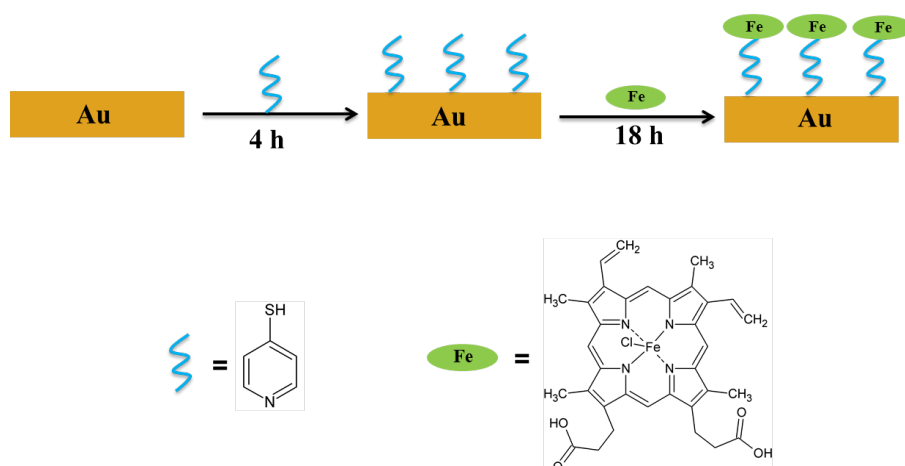


Figure S2. Workflow of the preparation of the MPy/hemin modified gold electrode.

Electrochemical characterization of a hemin modified gold disk electrode. We further investigated the electrochemical properties of the MPy/hemin modified Au using cyclic voltammetry (CV) at different scan rates. The anodic and cathodic peak currents increased linearly over a scan rate from 0.5 to 5 V s⁻¹ with correlation coefficients of 0.999 and 0.997 (Fig. S3), indicating that the redox reaction of the immobilized hemin is a surface-controlled process.² The surface coverage of hemin is estimated to be $\Gamma \approx 2.7 \times 10^{-12}$ mol cm⁻², while the hemin surface coverage on the nanostructured gold electrode is $\Gamma \approx 8.6 \times 10^{-12}$ mol cm⁻², using $\Gamma = Q/(nFA)$, where Q is the integrated charge across the reduction peak, n is the number of electrons in a faradic reaction, F is Faraday's constant, and A is the surface area of the

electrode.

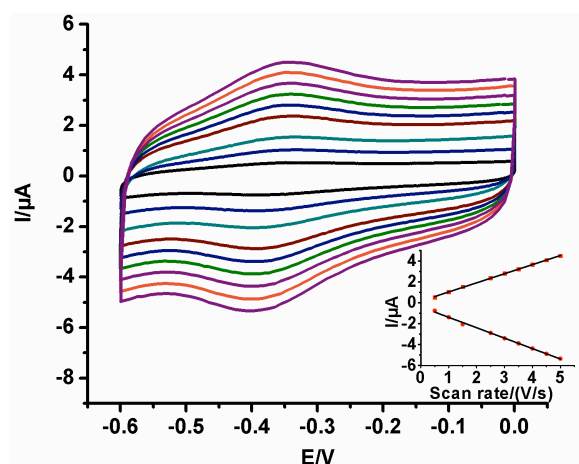


Figure S3. Cyclic voltammograms of an MPy/hemin modified Au electrode in 25 mM sodium phosphate buffer, pH 7.0 (argon saturated) at scan rates varying from 0.5 to 5 V s⁻¹ (inner to outer traces). Inset: redox peak currents versus scan rate.

Tabulated Raman assignments. In Table S1, assignments of the measured spectra from MPy modified nanostructured Au surfaces are listed.³ Preliminary assignments of the measured spectra of from MPy/hemin modified nanostructured Au surfaces are listed in Table S2.

Table S1. Raman band assignments from MPy modified nanostructured Au surfaces. The labels γ , β , and ν indicate out-of-plane bending, in-plane bending, and stretching modes, respectively. Laser power: 0.2 mW and 3 s integration time.

Band (cm ⁻¹)	Assignment ³
700	6a(a ₁), ν (C-S)+ β (C-C)
778	10b(b ₁), γ (C-H)
1000	1(a ₁), β (C-C-C)
1036	18a(a ₁), β (C-H)
1094	12(a ₁), β (C-C-C)+ ν (C-S)
1210	9a(a ₁), β (C-H)
1274	3(b ₂), β (C-H)
1492	19a(a ₁), ν (C=C/C=N)
1577	8b(b ₂), ν (C-C)
1608	8a(a ₁), ν (C-C)

Table S2. Raman band assignments from MPy/hemin modified nanostructured Au surfaces. Laser power: 0.2 mW and 10 s integration time. NA indicates not assigned. Hemin mode assignments ν_2 , ν_3 , ν_4 , ν_{10} , ν_{15} , ν_{20} , ν_{21} , and ν_{22} from Sanchez and Spiro⁷ and Hu, et al.⁸

<i>E</i> =-0.2 V			<i>E</i> =-0.5 V		
Band (cm ⁻¹)	Band area	Assignment	Band (cm ⁻¹)	Band area	Assignment
698	67797	MPy, 6a(a ₁)	697	53731	MPy, 6a(a ₁)
753	31141	hemin, ν_{15} (B _{1g}) ⁸	748	16538	hemin, ν_{15} (B _{1g}) ⁸
820	62381	NA	-	-	-
999	190534	MPy, 1(a ₁)	1008	90055	MPy, 1(a ₁)
1091	21430	MPy, 12(a ₁)	-	-	-
1123	51794	hemin, ν_{22} (A _{2g}) ⁷	1115	92383	hemin, ν_{22} (A _{2g}) ⁷
-	-	-	1163	21323	NA
-	-	-	1203	68978	NA
1236	471392	NA	1245	283345	NA
-	-	-	1271	24064	MPy, 3(b ₂)
1303	28550	hemin, ν_{21} (A _{2g}) ⁷	1305	140876	hemin, ν_{21} (A _{2g}) ⁷
1345	102876	hemin, ν_4 (A _{1g}), Fe ²⁺	1349	114378	hemin, ν_4 (A _{1g}), Fe ²⁺
1366	23812	hemin, ν_4 (A _{1g}), Fe ³⁺	-	-	-
1393	32577	hemin, ν_{20} (A _{2g}) ⁸ ; hemin+Py ⁶	1386	113532	hemin, ν_{20} (A _{2g}) ⁸ ; hemin+Py ⁶
1445	112956	hemin, ν_3 (A _{1g}) + MPy 19b(b ₂) ³	1447	331564	hemin, ν_3 (A _{1g}) + MPy 19b(b ₂) ³
1521	163211	NA	1533	251298	NA
1570	213342	hemin, ν_2 (A _{1g}) ⁷	1574	90939	hemin, ν_2 (A _{1g}) ⁷
1619	58160	hemin, ν_{10} (B _{1g}) ⁷	1607	215321	hemin, ν_{10} (B _{1g}) ⁷

Enhancement factor and surface density estimations. The mean and variance of the spatially averaged SERS enhancement factor are estimated from measurements of benzenethiol self-assembled monolayers on Au and Ag nanostructured surfaces and liquid neat benzenethiol. Since SERS is used for surface-enhanced Raman spectroscopy, the analytical enhancement factor for a specific vibrational mode at each measurement location (x_i , y_i) is estimated with $Y_i \approx (\kappa_i/N_{\text{SERS}})(\kappa_{\text{CR}}/N_{\text{CR}})^{-1}$, where κ_i and κ_{CR} are the integrated intensities from the SERS and conventional Raman measurements, respectively. N_{SERS} and N_{CR} are the number of molecules in the collection volume of each measurement, respectively. It should be noted that N_{SERS} is estimated from a monolayer on the SERS substrate surface. 200 SERS spectra from a Raman image were modeled using Lorentzian peak shapes and a cubic polynomial function for background subtraction. The κ_i of each band is estimated for each of the i measurements using modeled bands. The number of molecules within the collection volumes for each measurement of benzenethiol is $N_{\text{SERS}} = D_s A_s$, where D_s [unit: cm⁻²]

is the surface density of the molecules and A_s is the collection area of the microscope objective. The collection area can be estimated as $A_s \approx \pi R_d^2$, where R_d is the radius of the diffraction limited spot size of the microscope objective, which can be estimated from $2R_d = D_d \approx 1.27\lambda/\text{N.A.}$, where λ is the wavelength of the laser source, in this case $\lambda = 632.8$ nm, and N.A. is the numerical aperture of the microscope objective, in this case N.A. = 0.8. Therefore, $A_s \approx 1 \times 10^{-12} \text{ m}^2$, assuming that the spot size diameter is 1 μm . From the electrochemical measurements, the surface density of the hemin is $\Gamma \approx 9 \times 10^{-12} \text{ mol cm}^{-2} = 9 \times 10^{-8} \text{ mol m}^{-2}$. The number of hemin molecules in the spot size of the microscope objective is $\Gamma A_s N_A = (9 \times 10^{-8})(1 \times 10^{-12})(6 \times 10^{23}) \approx 5 \times 10^4$ hemin molecules. This value is small compared to the estimated number of molecules in a benzenethiol or MPy SAM on the nanostructured Au surface of approximately 3×10^6 molecules.⁵

References

1. S. Y Chen, J. G. Bomer, W. G. van der Wiel, E. T. Carlen, and A. van den Berg, *ACS Nano* 2009, 3, 3485-3492.
2. A. J. Bard, L. R. Faulkner, *Electrochemical Methods*. 2nd Ed., John Wiley & Sons, New York, 2001.
3. Varsanyi, G. *Vibrational Spectra of Benzene Derivatives*. Elsevier, Amsterdam, 1969.
4. Gui, J. Y.; Stern, D. A.; Frank, D. G.; Lu, F.; Zapien, D. C.; Hubbard, A. T. *Langmuir* 1991, 7, 955-963.
5. Le Thi Ngoc, L.; Jin, M.; Wiedemair, J.; van den Berg, A.; Carlen, E. T. *ACS Nano* 2013, 7, 5223-5234.
6. McMahon, J. J.; Baer, S.; Melendres, C. A. *J. Phys. Chem.* 1986, 90, 1572-1577.
7. Sanchez, L. A.; Spiro, T. G. *J. Phys. Chem.* 1985, 89, 763-768.
8. Hu, S.; Morris, I. K.; Singh, J. P.; Smith, K. M.; Spiro, T. G. *J. Am. Chem. Soc.* 1993, 115, 12446-12458.